Excerpt from the Proceedings of the 2011 COMSOL Conference in Stuttgart

Numerical Experiments for Thermally-induced Bending of Nematic Elastomers with Hybrid Alignment (HNEs)

Antonio DeSimone[1], Luciano Teresi[2*]
[1]SISSA-ISAS – International School for Advanced Studies, Trieste, Italy
[2*]LaMS – Modelling & Simulation Lab, Università Roma Tre, Roma, Italy
*corresponding author: LaMS, Via Corrado Segre, 6, 00146 Roma, Italy;
e-mail *teresi@uniroma3.it*

Abstract: The nematic elastomers with hybrid alignment (HNEs) exhibit large anisotropic and non homogeneous volume changes, which can induce noticeable changes in their configuration. Here, we deal with LCEs having hybrid alignment (HNEs), that is, fabricated with a given non-homogeneous nematic orientation. For such a materials, permanent distortions induced by deswelling can be compensated by those resulting from cooling below T_N; it results the possibility of producing temperature-driven actuators.

Keywords: Liquid crystal elastomer, nematic-isotropic phase transition, swelling.

1 Introduction

Liquid crystal elastomers (LCEs) possess very interesting properties stemming from the interaction between liquid crystal order and rubber elasticity [1]. For such materials, thermally-induced phase transition from the isotropic to the nematic phase may induce very large distortions, see Figure 1, which, in turn, can affect the overall configuration of a macroscopic specimen.

A particular class of LCEs features two sorts of large anisotropic phase transitions: the first one is a deswelling due to solvent evaporation, that manifests during preparation; the second one, thermally induced, is due to an isotropic-nematic phase transition. Both phenomena can produce noticeable changes of configuration in a given specimen, but, while deswelling induces permanent changes, the isotropic-nematic phase transitions are reversible: cooling below a transition temperature T_N produces the nematic phase, whose effects become larger as the temperature decreases; heating above T_N restores the isotropic one.

Here, we deal with LCEs having hybrid alignment (HNEs), that is, fabricated with a given non-homogeneous nematic orientation. For such a materials, permanent distortions induced by deswelling can be compensated by those resulting from heating; it results the possibility of producing temperature driven actuators. See [3] for a detailed description about preparation of HNEs, and experimental results.

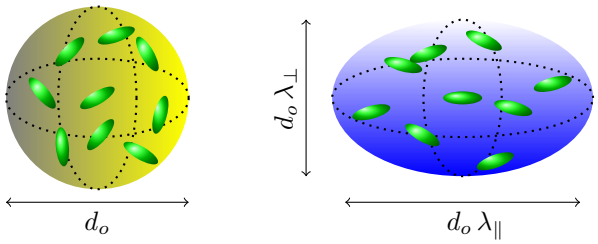

Figure 1: If the stress-free shape of a mesoscopic chunk of LCE is a spherical ball when the appended mesogens are in the disordered, isotropic phase (left), its stress-free shape in the ordered, nematic phase is a prolate spheroid whose polar axis is aligned with the prevailing mesogen direction. LC molecules are caricatured grossly out of scale.

2 The physical model

We model the HNEs in the framework of 3D incompressible non-linear elasticity with large distortions [2]. We represent the nematic orientation with the nematic tensor field[1] $\mathbf{N} := \mathbf{n} \otimes \mathbf{n}$, with $\mathbf{n}$ a unit vector field ($|\mathbf{n}| = 1$); the elastomer *distortions* we deal with are *uniaxial stretch* aligned with mesogen orientation $\mathbf{N}$:

$$\mathbf{U}_o = \lambda_\parallel \, \mathbf{N} + \lambda_\perp \, (\mathbf{I} - \mathbf{N}) \,, \tag{2.1}$$

where $\mathbf{I}$ is the identity, and the scalars $\lambda_\parallel$, $\lambda_\perp$ represent the magnitude of the strains along $\mathbf{n}$, and in the plane orthogonal to $\mathbf{n}$, see Fig.(1). We shall use (2.1) to represent both swelling- and temperature-induced distortions. A key feature of HNEs is that they can be fabricated with a given, possibly non-homogeneous, nematic orientation $\mathbf{N}$; moreover, the stretches $\lambda_\parallel$, $\lambda_\perp$ are sensible to solvent evaporation and temperature.

2.1 Swollen Nematic Gels

We consider a material whose state is described, apart from a displacement field, by the pair (ϑ, v): the first parameter $\vartheta = T/T_N$ is the ratio between the actual temperature T, and the *transition temperature* T_N; the second one measures the volume change occurring during *deswelling*.

Our specimen is prepared in the wet-nematic state $(\vartheta_n, 1)$, with $\vartheta_n < 1$ the preparation temperature, and undergoes two phase transitions: deswelling at constant temperature ϑ_n, until a fully dry state with $v = v_d$; heating at constant deswollen ratio v_d, until a temperature $\vartheta > 1$, see state diagram in Fig.(2). Given the four points in the diagram

$$a = (1, 1) \,, \; b = (1, v_d) \,, \; c = (\vartheta_n, 1) \,, \; d = (\vartheta_n, v_d) \,,$$

they can be connected with four maps: $\mathbf{D}^i(v)$, $\mathbf{D}^n(v)$ represent deswelling distortions (at constant temperature), in the isotropic and in the nematic state, respectively; $\mathbf{A}^w(\vartheta)$, $\mathbf{A}^d(\vartheta)$ represent the cooling distortions (at constant deswelling) in the wet and in the dry state, respectively, see Fig. (2). The four maps satisfy:

$$\mathbf{D}^i(1) = \mathbf{I} \,, \; \mathbf{D}^n(1) = \mathbf{I} \,, \; \mathbf{A}^w(1) = \mathbf{I} \,, \; \mathbf{A}^d(1) = \mathbf{I} \,;$$

moreover, deswelling is accompanied to volume variation, while isotropic-nematic transition is volume preserving; thus: $\det \mathbf{D}^i(v) = \det \mathbf{D}^n(v) = v$, $\det \mathbf{A}^w(\vartheta) = \det \mathbf{A}^d(\vartheta) = 1$.

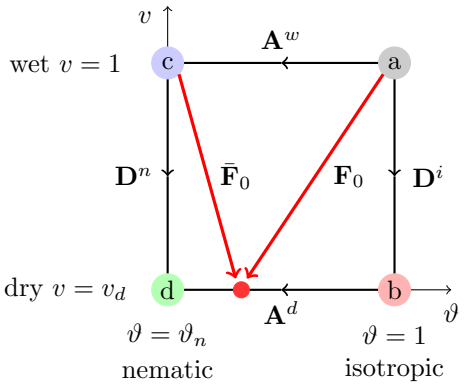

Figure 2: State diagram showing the phase transitions we consider.

A distortion from point a to a generic state (ϑ, v) is described by the map $\mathbf{F}_o$

$$\mathbf{F}_o(\vartheta, v) = \mathbf{A}^d(\vartheta) \, \mathbf{D}^i(v) \,. \tag{2.2}$$

In order to have the point c as reference, we consider the map $\bar{\mathbf{F}}_o$

$$\bar{\mathbf{F}}_o(\vartheta, v) = \mathbf{F}_o(\vartheta, v) \, \mathbf{A}^w(\vartheta_n)^{-1} \,. \tag{2.3}$$

From

$$\mathbf{A}^w(\vartheta_n) = \mathbf{D}^n(v)^{-1} \, \mathbf{A}^d(\vartheta_n) \, \mathbf{D}^i(v) \,, \tag{2.4}$$

it follows that, to describe a path starting from c, only $\mathbf{A}^d$ and $\mathbf{D}^n$ are needed:

$$\begin{aligned} \bar{\mathbf{F}}_o(\vartheta, v) &= \mathbf{A}^d(\vartheta) \, \mathbf{D}^i(v) \, [\mathbf{D}^n(v)^{-1} \, \mathbf{A}^d(\vartheta_n) \, \mathbf{D}^i(v)]^{-1} \\ &= \mathbf{A}^d(\vartheta) \, \mathbf{A}^d(\vartheta_n)^{-1} \, \mathbf{D}^n(v) \,. \end{aligned} \tag{2.5}$$

It is worth noting that equation (2.5) implies that

$$\begin{aligned} \vartheta = \vartheta_n \,, v = 1 \quad &\Rightarrow \bar{\mathbf{F}}_o = \mathbf{I} \,, \\ \vartheta = \vartheta_n \,, v < 1 \quad &\Rightarrow \bar{\mathbf{F}}_o = \mathbf{D}^n(v) \,, \\ \vartheta = 1 \,, v < 1 \quad &\Rightarrow \bar{\mathbf{F}}_o = \mathbf{A}^d(\vartheta_n)^{-1} \, \mathbf{D}^n(v) \,. \end{aligned} \tag{2.6}$$

[1] Not to be confused with the nematic order tensor. The nematic tensor $\mathbf{N}$ is the proper kinematics descriptor as it accounts only for the orientation of molecules, without discriminating between $+\mathbf{n}$ and $-\mathbf{n}$.

The distortions $\mathbf{D}^n(v)$ and $\mathbf{A}^d(\vartheta)$ are uniaxial stretches, sharing the same representation formula (2.1); here, we shall denote with $\alpha(v)$ and $\lambda(\vartheta)$ the swelling- and temperature-induced stretches, respectively:

$$\begin{aligned} \mathbf{D}^n(v) &= \alpha_\parallel(v)\,\mathbf{N} + \alpha_\perp(v)\,(\mathbf{I}-\mathbf{N})\,, \\ \mathbf{A}^d(\vartheta) &= \lambda_\parallel(\vartheta)\,\mathbf{N} + \lambda_\perp(\vartheta)\,(\mathbf{I}-\mathbf{N})\,, \end{aligned} \tag{2.7}$$

where, as consequence of volume constraints:

$$\alpha_\parallel(v)\,\alpha_\perp^2(v) = v\,, \quad \lambda_\parallel(\vartheta)\,\lambda_\perp^2(\vartheta) = 1\,. \tag{2.8}$$

Moreover, given (2.7), $\bar{\mathbf{F}}_o(\vartheta, v)$ admits a straightforward representation

$$\bar{\mathbf{F}}_o(\vartheta, v) = \frac{\lambda_\parallel(\vartheta)\,\alpha_\parallel(v)}{\lambda_\parallel(\vartheta_n)}\,\mathbf{N} + \frac{\lambda_\perp(\vartheta)\,\alpha_\perp(v)}{\lambda_\perp(\vartheta_n)}\,(\mathbf{I}-\mathbf{N})\,. \tag{2.9}$$

Let $\mathbf{F}$ denote a deformation with respect to the wet-nematic state (point c), and let $\mathbf{C} = \mathbf{F}^\top\mathbf{F}$ be the associated strain; the elastic deformation $\mathbf{F}^e$ and the elastic strain $\mathbf{C}^e$ are given by

$$\mathbf{F}^e = \mathbf{F}\,\bar{\mathbf{F}}_o^{-1}\,, \quad \mathbf{C}^e = (\mathbf{F}^e)^\top\,\mathbf{F}^e = \bar{\mathbf{F}}_o^{-\top}\mathbf{C}\,\bar{\mathbf{F}}_o^{-1}\,; \tag{2.10}$$

we consider a Neo-Hookean elastic energy density

$$\begin{aligned} &\phi = \tfrac{1}{2}\,\mu\,(\mathbf{C}^e\cdot\mathbf{I} - 3) = \tfrac{1}{2}\,\mu\,(\mathbf{C}\cdot\mathbf{C}_o^{-1} - 3)\,, \\ &\det(\mathbf{C}_o) = v^2, \end{aligned} \tag{2.11}$$

with μ the shear modulus, and $\mathbf{C}_o$ the distortional strain induced by $\bar{\mathbf{F}}_o$:

$$\mathbf{C}_o(\vartheta, v) = \bar{\mathbf{F}}_o^\top(\vartheta, v)\,\bar{\mathbf{F}}_o(\vartheta, v)\,. \tag{2.12}$$

It follows from (2.11) that $\mathbf{C} = \mathbf{C}_o$ is a minimum; we can easily verify that the wet-nematic state realizes the reference configuration:

$$(\vartheta, v) = (\vartheta_n, 1) \;\Rightarrow\; \bar{\mathbf{F}}_o = \mathbf{I} \;\Rightarrow\; \mathbf{C}_o = \mathbf{I} \;\Rightarrow\; \mathbf{C} = \mathbf{I}\,;$$

moreover, to $\mathbf{C}_o \propto \mathbf{I}$ there correspond a homogenous state, that is, a *flat* configuration; thus, a noteworthy consequence of (2.9) is that it can be used to determine the temperature ϑ_f corresponding to such a flat state. Being $\mathbf{C}_o = \bar{\mathbf{F}}_o^2$, the condition $\mathbf{C}_o \propto \mathbf{I}$ is equivalent to $\bar{\mathbf{F}}_o \propto \mathbf{I}$; it follows that ϑ_f satisfies

$$\frac{\lambda_\parallel(\vartheta_f)\,\alpha_\parallel^d}{\lambda_\parallel(\vartheta_n)} = \frac{\lambda_\perp(\vartheta_f)\,\alpha_\perp^d}{\lambda_\perp(\vartheta_n)}\,. \tag{2.13}$$

Actually, from experimental data [3], we know the deswelling distortions at the completely dry state, and the expressions relating the temperature to the cooling distortions, that is, we know:

$$\begin{aligned} &\alpha_\parallel^d = \alpha_\parallel(v_d)\,, \quad \alpha_\perp^d = \alpha_\perp(v_d)\,, \\ &\lambda_\parallel(\vartheta) = \begin{cases} 1 + \beta(1-\vartheta)^a\,, & \vartheta \in (\vartheta_n, 1)\,; \\ 1\,, & \vartheta \geq 1\,. \end{cases} \end{aligned} \tag{2.14}$$

By using the relations between $\lambda_\parallel$, $\lambda_\perp$, equation (2.13) may be solved explicitly for $\lambda_f := \lambda_\parallel(\vartheta_f)$:

$$\lambda_f = \lambda_\parallel(\vartheta_n)\left(\frac{\alpha_\perp^d}{\alpha_\parallel^d}\right)^{2/3}, \; \mathbf{F}_o(\vartheta_f, v_d) = v_d^{1/3}\,\mathbf{I}\,. \tag{2.15}$$

Then, inverting the function $\vartheta \mapsto \lambda_\parallel(\vartheta)$, we can compute the flat temperature

$$\vartheta_f = 1 - \left(\frac{\lambda_f - 1}{\beta}\right)^{1/a}\,. \tag{2.16}$$

We note that the nematic orientation $\mathbf{N}$ does not enter in the formula for the flat temperature; nonetheless, it plays a key role for the stress state realized in configurations different from the flat ones.

3 Model implementation

We consider as reference configuration a parallelepipedal body $\mathscr{B}$ of sides $L \times W \times H$ representing the HNE at the preparation state (wet-nematic; point c in Fig.(2)). We denote with $\{o; x, y, z\}$ a Cartesian frame having its origin o at the center of $\mathscr{B}$, and the three axes aligned with L, W, and H, respectively. We assume the nematic tensor $\mathbf{N}$ to lie in the plane x, z, and having a linear variation along z, with $\mathbf{N}$ parallel to z at $z = -H/2$, and $\mathbf{N}$ parallel to x at $z = H/2$. The specimen is unloaded, clamped at the face $x = -L/2$ and free on other faces.

We implement the balance equations of nonlinear elasticity in weak form, using the volumetric-deviatoric decomposition of the deformation measures, and adopting a mixed method. Thus, we have as independent variables the displacement vector $\mathbf{u}$, and the pressure p; given $\mathbf{F} = \mathbf{I} + \nabla\mathbf{u}$, we

consider the following relaxed strain energy density: $\phi_r = \phi_s + \phi_v$, with

$$\begin{aligned}
&\phi_s = \tfrac{1}{2}\,\mu\,(\mathbf{C}_s \cdot \mathbf{C}_o^{-1} - 3) && \text{isochoric energy;}\\
&\phi_v = \tfrac{k}{2}\,(J - v)^2 && \text{volumetric energy;}\\
&\mathbf{C}_s = (v/J)^{2/3}\,\mathbf{C}\,, && \text{unimodular part of } \mathbf{C};\\
&p = -k\,(J - v)\,, && \text{pressure;}\\
&J = \det(\mathbf{F})\,, && \text{volume change;}
\end{aligned} \tag{3.17}$$

and k the bulk modulus. The reference and the actual stress are then given by

$$\begin{aligned}
&\mathbf{S} = 2\,\mathbf{F}^e\,\mathbf{S}_{sc}\,\bar{\mathbf{F}}_o^{*} - p\,\mathbf{F}^{*},\\
&\mathbf{T} = \mathbf{S}\,(\mathbf{F}^{*})^{-1}
\end{aligned} \tag{3.18}$$

with $\mathbf{A}^{*} = \mathbf{A}^{-\top}$ denoting the cofactor of $\mathbf{A}$, and

$$\mathbf{S}_{sc} = \frac{\partial \psi_s}{\partial \mathbf{C}^e} = \frac{1}{2}\,\mu\,J_e^{-2/3}\left(\mathbf{I} - \frac{1}{3}\,\mathrm{tr}(\mathbf{C}^e)\,(\mathbf{C}^e)^{-1}\right), \tag{3.19}$$

where $J_e = \det(\mathbf{F}^e) = J/v$. It follows

$$\begin{aligned}
&\mathbf{S} = \mu\,v\,\mathbf{F}\,\mathbf{C}_o^{-1} - p\mathbf{F}^{*}\,;\\
&\mathbf{T} = \mu\,\frac{1}{J_e}\,\mathbf{F}_e\,\mathbf{F}_e^{\top} - p\,\mathbf{I}\,.
\end{aligned} \tag{3.20}$$

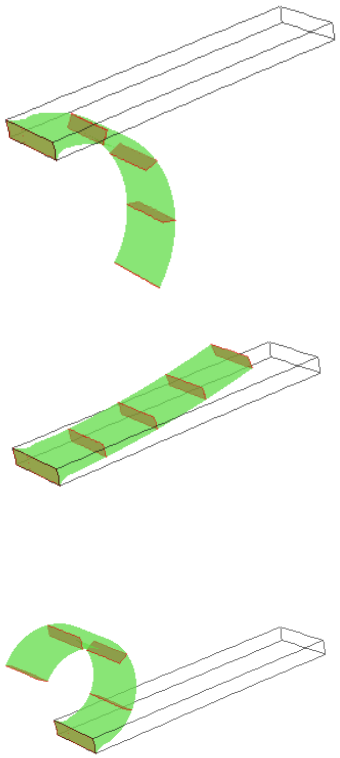

Figure 3: Results from numerical experiments. From top to bottom: dry state at preparation temperature ϑ_n; nearly flat state at $\vartheta \sim \vartheta_f$; isotropic state at $\vartheta = 1$. Wireframe renders the preparation state; five cross sections highlight bending.

3.1 Balance equations

Balance equations are implemented using a mixed L2-L1 method, that is using second- and first-order Lagrangian shape functions for the displacement and the pressure, respectively. The problem is then stated follows: find a displacement $\mathbf{u}$, and a pressure p such that, for all test function $\widetilde{\mathbf{u}}$, and $\widetilde{p}$ it holds:

$$\begin{aligned}
&\int_{\mathscr{B}} \left(-\mathbf{S} \cdot \nabla\widetilde{\mathbf{u}} + \mathbf{f} \cdot \widetilde{\mathbf{u}} \right) = 0\,,\\
&\int_{\mathscr{B}} (\frac{p}{k} + J - v) \cdot \widetilde{p} = 0\,,
\end{aligned} \tag{3.21}$$

with $\mathbf{u} = 0$ at $x = -L/2$. From (2.12), (3.20) it follows that the reference stress is a function of the independent variables $\mathbf{u}$ and p, and of the state variables (ϑ, v):

$$\mathbf{S} = \mathbf{S}(\mathbf{u}, p; \vartheta, v)\,. \tag{3.22}$$

Thus, we can solve (3.21) for $\mathbf{u}$ and p, using the pair (ϑ, v) as parameters; in particular, using the parametric solver, we first simulate deswelling, by solving a sequence of N elastic problems corresponding to (ϑ_n, v_i), with $v_1 = 1$, $v_N = v_d < 1$. The final solution we obtain corresponds to the dry-nematic state, and it is used as initial data to simulate the heating process; thus, we solve another sequence of N elastic problems for (ϑ_i, v_d), with $\vartheta_1 = \vartheta_n$, $\vartheta_N = 1$.

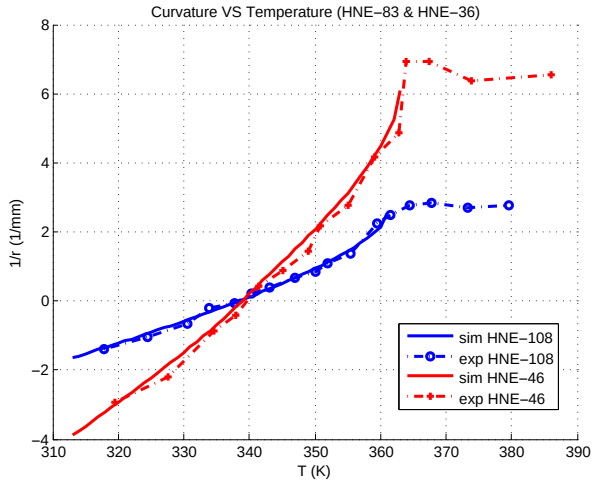

Figure 4: Curvature versus temperature. The plot shows the results from numerical (solid line) and actual (dotted line with marker) experiments for two similar specimens having different thickness and length ($H = 108 \sim 46\,\mu m$).

4 Results

We simulated the behavior of different parallelepipedal specimens under deswelling and heating, with the goal of reproducing actual experiments. Fig.(3) shows three snapshots from numerical experiments: the wireframe renders the preparation state of the specimen undergoing a very large bending during deswelling (top) and a counter-bending during heating (top). Fig.(4) shows curvature versus temperature for two same specimens differing in height H and L: numerical results (solid line) is benchmarked against experimental data (dotted line with "o" and "+" markers) as published in [3]. As expected, curvature is very sensitive to thickness H, whose values are reported in the figure, and is not to length L or width W. Values of parameters used in our simulations are given in table 1.

5. Conclusion

The outcome from the numerical implementation of the present problem is twofold: at first, we assess the effectiveness of the underlying physical model and we tune the material parameters which are difficult to measure; then, we can predict distortion-induced shape formation in specimen with non trivial initial configuration.

Table 1: Parameter list

Symbol	Value	Description
L	$2000 \sim 1400\,\mu m$	length
W	$500\,\mu m$	width
H	$108 \sim 46\,\mu m$	thickness (wet)
v_d	0.45	wet/dry vol. ratio
$\alpha^d_{\parallel}$	0.82	$\alpha_{\parallel}$ at v_d
$\alpha^d_{\perp}$	0.74	$\alpha_{\perp}$ at v_d
a	0.5	parameter for (2.14)
β	0.68	parameter for (2.14)
T_N	363 K	transition temp.
T_o	313 K	preparation temp.

Results from numerical and actual experiments agree very well, as Fig.(4) shows; thus, we are confident that our numerical simulation could be useful in designing micro actuator based on HNEs prior to their actual production.

Acknowledgements We wish to acknowledge Kenji Urayama for having introduced us into the phenomenology of HNEs, for many helpful discussions on the topic, and for sharing key experimental data; we also acknowledge the Department of Materials Chemistry, Kyoto University, for offering kind hospitality during our past visit.

References

[1] K. Urayama, Selected Issues in Liquid Crystal Elastomers and Gels. *Macromolecules* 40, 2277–2288 (2007)

[2] A. DeSimone, L. Teresi, Elastic energies for nematic elastomers. *Eur. Phys. J. E* 29, 191–204 (2009)

[3] Y. Sawa, K. Urayama, T. Takigawa, A. DeSimone, L. Teresi, Thermally Driven Giant

Bending of Liquid Crystal Elastomer Films with Hybrid Alignment. *Macromolecules* 43, 4362–4369 (2010)